Ocean Dynamics (2015) 65:1079–1093
DOI 10.1007/s10236-015-0853-7

The use of a flow field correction technique for alleviating the North Atlantic cold bias with application to the Kiel Climate Model

Annika Drews[1] · Richard J. Greatbatch[1] · Hui Ding[1] · Mojib Latif[1] · Wonsun Park[1]

Received: 5 November 2014 / Accepted: 21 May 2015 / Published online: 20 June 2015

Abstract The North Atlantic cold bias, associated with the misplacement of the North Atlantic Current (NAC) and typically extending from the surface to 1000 m depth, is a common problem in coupled models that compromises model fidelity. We investigate the use of a flow field correction (FFC) to adjust the path of the NAC and alleviate the cold bias. The FFC consists of three steps. First, climatological potential temperature (T) and salinity (S) fields for use with the model are produced using a three-dimensional restoring technique. Second, these T, S fields are used to modify the momentum equations of the ocean model. In the third stage, the correction term is diagnosed to construct a flow-independent correction. Results using the Kiel Climate Model show that the FFC allows the establishment of a northwest corner, substantially alleviating the subsurface cold bias. A cold bias remains at the surface but can be eliminated by additionally correcting the surface freshwater flux, without adjusting the surface heat flux seen by the ocean model. A model version in which only the surface fluxes of heat and freshwater are corrected continues to exhibit the incorrect path of the NAC and a strong subsurface bias. We also show that the bias in the atmospheric circulation is reduced in some corrected model versions. The FFC can be regarded as a way to correct for model error, e.g. associated with the deep water mass pathways and their impact on the large-scale ocean circulation, and unresolved processes such as eddy momentum flux convergence.

Keywords North Atlantic cold bias · Northwest corner · Empirical correction techniques · North Atlantic Current

Responsible Editor: Jinyu Sheng

This article is part of the Topical Collection on *Atmosphere and Ocean Dynamics: A Scientific Workshop to Celebrate Professor Dr. Richard Greatbatch's 60th Birthday, Liverpool, UK, 10–11 April 2014*

✉ Annika Drews
adrews@geomar.de

[1] GEOMAR Helmholtz Centre for Ocean Research Kiel, Düsternbrooker Weg 20, 24105, Kiel, Germany

1 Introduction

Climate models still suffer from large systematic errors. One prominent example is the incorrect path of the Gulf Stream and the North Atlantic Current (NAC) and the corresponding lack of penetration of warm, salty water into the so-called "northwest corner" east of Newfoundland (see Lazier 1994). Typically, the model NAC extends zonally from Newfoundland to Europe, while in observations, the NAC turns northward, following the bottom topography associated with the Grand Banks of Newfoundland from 40° to 50° N and flowing into the northwest corner, before it turns eastward again. The misplacement of the NAC is associated with cold sea surface temperatures (SSTs) east and south of Newfoundland: the typical North Atlantic cold bias (see Wang et al. 2014; Flato et al. 2014). The associated error in SST can locally be as much as 10 °C. An inevitable consequence of the cold bias is the increased importance of salinity for controlling density in the subpolar North Atlantic, calling into question mechanisms for low frequency variability in the models (e.g. Delworth et al. 1993; Born and Mignot 2012; Ba et al. 2013).

The misplacement of the NAC is also a feature of ocean-only models driven by a specified atmosphere (see, e.g. Eden et al. 2004; Bryan et al. 2007; Hecht and Smith 2008).

The erroneous circulation is clearly revealed in sea surface height (SSH) in the models. In particular, the path of the North Atlantic Current is too zonal and the northwest corner is missing, as in the coupled models. Going to very high horizontal resolution (e.g. 1/20th of a degree) has been shown to alleviate the bias in some models (Figure 19 in Behrens 2013; Mertens et al. 2014). However, increasing the horizontal resolution may not, of itself, be a guarantee that the bias in a coupled model is reduced, as shown by the work of Delworth et al. (2012) and Griffies et al. (2014) where the ocean model horizontal resolution approaches 1/10th degree.

The region centred on the northwest corner has long been thought to exercise an influence on European weather and climate (e.g. Ratcliffe and Murray 1970; Rodwell et al. 1999; Rodwell and Folland 2002; Folland et al. 2012; Scaife et al. 2014). In models that exhibit the cold bias, the surface heat flux in this region has the wrong sign, as the atmosphere warms the ocean to counter the bias (see Section 2). Given that the surface heat flux is thought to be important in the dynamics of the storm track (Hoskins and Valdes 1990; Brayshaw et al. 2011), it is possible that the presence of the cold bias compromises the ability of models to reproduce the correct atmospheric variability over the North Atlantic and, in particular, to produce an accurate response in forecast models to either remote forcing (e.g. from the tropics) or to local SST anomalies. Indeed, Scaife et al. (2014) report significantly improved skill at forecasting the winter North Atlantic Oscillation (NAO; see Greatbatch 2000 and Hurrell et al. 2003 for reviews of the NAO) using an improved coupled forecast model in which the cold bias is significantly reduced (Scaife et al. 2011, Scaife, personal communication). Furthermore, it is known that the cold bias is responsible for a bias in the mean atmospheric circulation over the North Atlantic in the HiGEM model from the UK Met Office (Keeley et al. 2012). In particular, the winter circulation over the North Atlantic in the model is too zonal and too strong westerly (a bias of roughly one standard deviation positive in the NAO).

Concerning the dynamics of the northwest corner, diagnostic model studies, in which the ocean density is specified, suggest that the deep circulation is an important factor for driving transport through vortex stretching (e.g. Greatbatch et al. 1991), as do studies using prognostic ocean models in which the deep water characteristics are changed (Gerdes and Köberle 1995). There is also evidence that the lateral flux of momentum by mesoscale eddies is important for driving circulation in the northwest corner region (Greatbatch et al. 2010). The latter is poorly represented in coarse resolution climate and forecast models (such models usually include a lateral eddy viscosity term that fluxes momentum down, rather than up, the mean gradient). It follows that at least two sources of error in the ocean model component of a coupled climate model could contribute to the circulation bias: error in the formation and pathways of deep water (both North Atlantic Deep Water and Antarctic Bottom Water) and error in the representation of mesoscale eddies and, in particular, the lateral flux of momentum by eddies.

In this article, we describe the use of empirical techniques to correct for the missing northwest corner in models. The corrections are implemented and examined in a coupled atmosphere/ocean/sea ice model (the Kiel Climate Model, KCM; Park et al. 2009). These techniques can be viewed as a simple way to parameterise missing physical processes in the models and to correct for model error. The first of these corrections is a "flow field correction" that is an adaption of the "corrected-prognostic" method introduced by Eden et al. (2004). The flow field correction corrects the oceanic flow field by adjusting the pressure field using a non-flow interactive correction. The method is derived from the semi-prognostic method of Sheng et al. (2001) and Greatbatch et al. (2004) and uses climatological hydrographic data to construct a correction term that adjusts the path of the North Atlantic Current into a more realistic position. The semi-prognostic method has been used previously in a fully coupled climate model (Weese and Bryan 2006) with promising results. Here, we go further by making the correction non-flow interactive. The second correction technique corrects for remaining biases in SST and sea surface salinity (SSS) by adding a non-interactive correction to the surface heat and freshwater fluxes, respectively, as in traditional "flux adjustment", also referred to as "flux correction" (e.g. as used by Manabe and Stouffer 1988; Sausen et al. 1988). Several different experiments are conducted to examine the role of each correction term from which the fundamental importance of the flow field correction emerges.

The paper is arranged as follows. The KCM and the characteristics of its errors in the North Atlantic are described in Section 2, while Section 3 concentrates on the correction techniques and their implementation in the KCM. Section 4 then presents the results and Section 5 provides a summary and discussion.

2 The Kiel Climate Model: the model configuration and the cold bias in the KCM

For our experiments, we use the Kiel Climate Model (Park et al. 2009). The atmospheric component is ECHAM5 (Roeckner et al. 2003) with T31 horizontal resolution ($\approx 3.75° \times 3.75°$) and 19 vertical levels with a lid at 10 hPa. OASIS3 (Valcke 2006, 2013) couples the atmospheric model to the ocean–sea ice model, in this case NEMO (Madec 2008) on the ORCA2 grid ($\approx 2° \times 2°$, 31 vertical levels). In the standard configuration, no form of

Table 1 The model experiments. Interactive run refers to the length of the model runs that use a flow-interactive correction, of which the last 50 years were used to construct the correction fields for the model runs with the non-interactive corrections (see text for details)

Experiment ID	Flow field correction	Surface flux correction	Interactive run (years)
CTRL	No	No	–
C-FFC	Yes	No	549
C-FS0	Yes	Freshwater	249
C-FST	Yes	Heat and freshwater	549
C-0ST	No	Heat and freshwater	549

flux correction or anomaly coupling is used. In all simulations, greenhouse gas concentrations are kept constant at a late twentieth century level (CO_2 = 348 ppmv). Further details are described in Park et al. (2009).

With the standard configuration (referred to as Experiment CTRL in Table 1), the model is initialised on January 1 with the Levitus monthly potential temperature (T) and salinity (S) climatology (Levitus et al. 1998) in the ocean component and the atmospheric component using a short run in which the Levitus SST is specified at the lower boundary. The North Atlantic cold bias develops quickly and is fully formed after only 30 years of integration (not

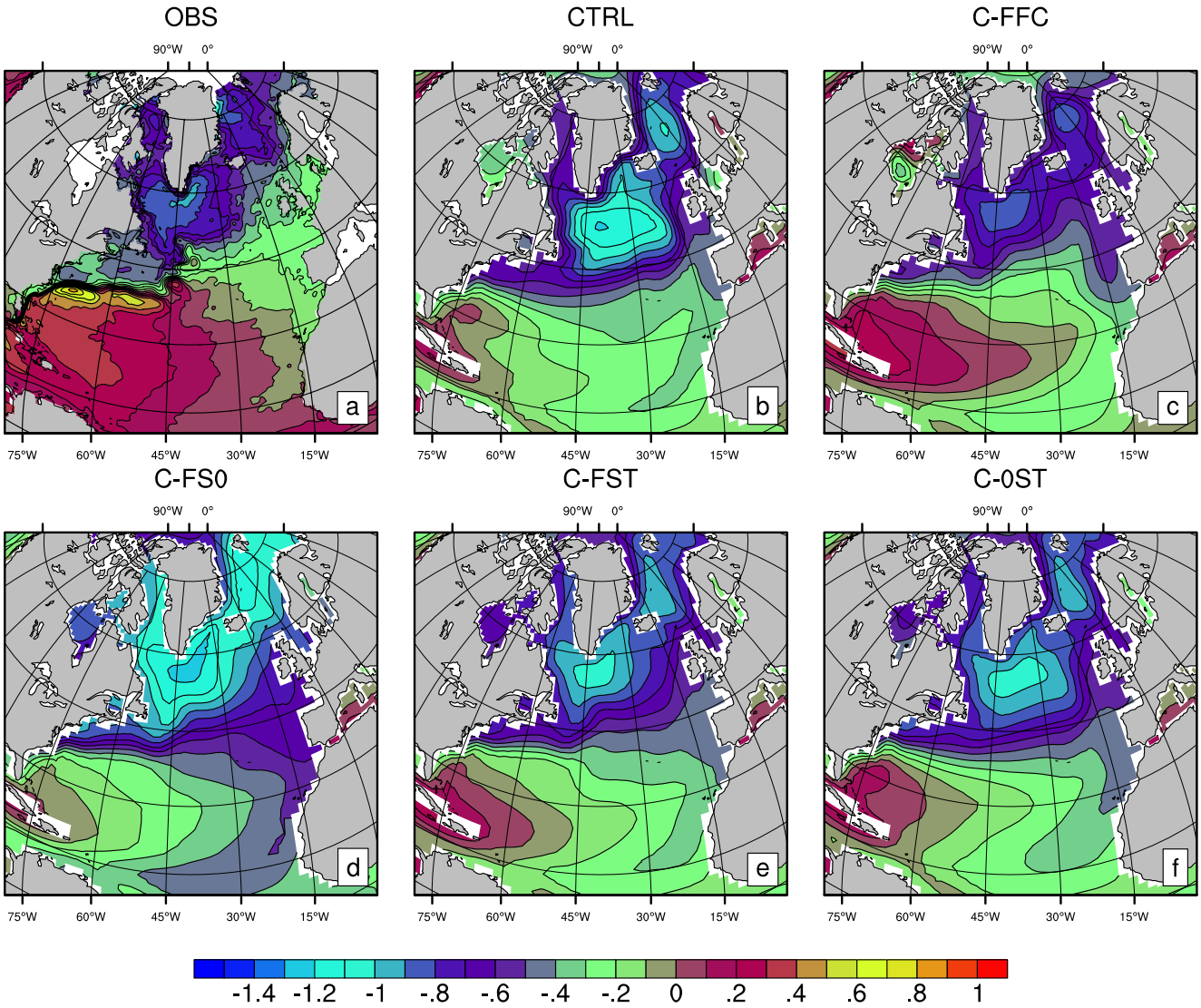

Fig. 1 Mean sea surface height (m) **a**) as observed (AVISO, 1993–2008), **b** of the control simulation CTRL, and of Experiments **c** C-FFC, **d** C-FS0, **e** C-FST and **f** C-0ST. In the case of all figure panels, the global mean sea level is removed. Longitude/latitude intervals are 15° in all figures

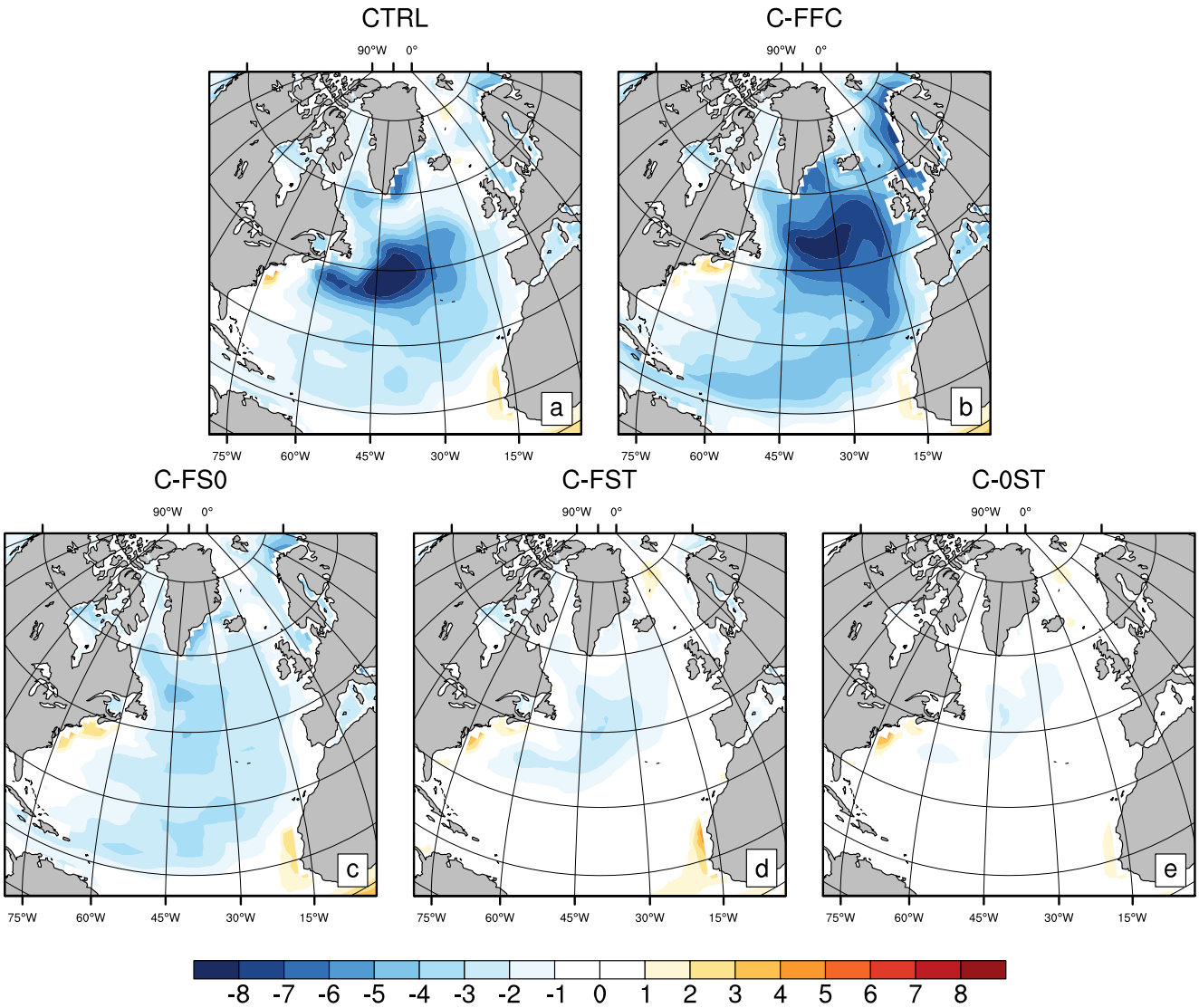

Fig. 2 Mean SST bias (°C) of **a** the KCM control experiment (CTRL), **b** Experiment C-FFC, **c** Experiment C-FS0, **d** Experiment C-FST and **e** Experiment C-0ST, using the WOA (Levitus et al. 1998) as the reference

shown). The subsequent analysis uses years 31–199 of this integration. The erroneous circulation is illustrated in Fig. 1 where the mean SSH from the control run (CTRL; Fig. 1b) is compared with satellite observations (Fig. 1a).[1] In Fig. 1a, the northwest corner east of Newfoundland is clearly evident (note the northward bending of the height contours into this region), a feature that is completely missing from Experiment CTRL. The absence of water of tropical origin in the northwest corner leads to a substantial cold bias in the model compared to Levitus climatology (Levitus et al. 1998) whose amplitude reaches up to 10 °C (see Fig. 2a). Figure 3 shows a vertical section along 43° N passing through the core of the cold bias from which it can be seen that the cold bias extends to 1000 m depth. This is not surprising given that the North Atlantic Current extends to at least 1000 m depth in observations east of Newfoundland (see Figure 1 in Schott et al. 2006). One effect of the cold bias is to reverse the direction of the surface heat flux compared to observations (at least in the centre of the region occupied by the bias), so that instead of the ocean heating the atmosphere in this region (Fig. 4a), the atmosphere warms the ocean as it tries to counter the bias (Fig. 4b). In the KCM, this error in the surface heat flux is as great as 150 W/m^2. The error in the surface heat flux leads to an erroneous bump in the poleward heat transport centred at $\sim$ 50° N due to the input of heat from the atmosphere over the region of the cold bias (see Fig. 5, black line; discussed further in Section 4). In the Labrador Sea, too

[1]The altimeter products were produced by Ssalto/Duacs and distributed by Aviso, with support from Cnes (http://www.aviso.altimetry.fr/duacs/).

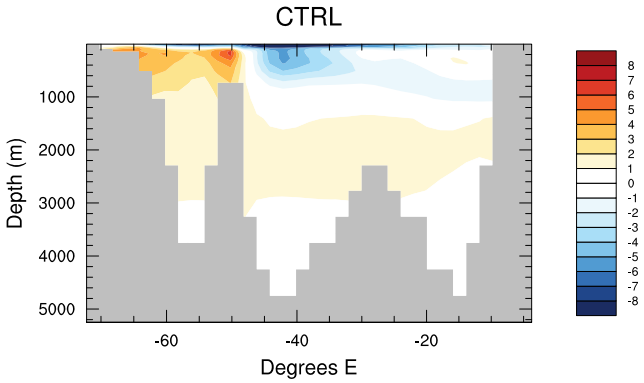

Fig. 3 Mean subsurface potential temperature (°C) bias along 43° N from Experiment CTRL, passing through the core of the cold bias and referenced to the WOA (Levitus et al. 1998)

cold SSTs encourage an increase in sea ice compared to observations (see Fig. 6b), which inhibits deep water formation and shifts the centre of convection to a location south of Greenland, disagreeing with observations (compare Fig. 6a, b where the winter mean mixed layer deep is plotted as a proxy for deep convection, and also Ba et al. (2013)). The cold bias is accompanied by a fresh bias as can be seen in Fig. 7a, where the sea surface salinity bias is shown.

The atmospheric errors are exemplarily illustrated for the winter season (December/January/February (DJF)) by the bias in sea level pressure (SLP), shown in Fig. 8a. It can be seen that the error in SLP can be as much as 10 hPa in the North Atlantic sector and projects onto the East Atlantic pattern (Barnston and Livezey 1987). This is rather different from the bias reported by Keeley et al. (2012) in the HiGEM model. In that case, the bias more closely resembles the positive phase of the North Atlantic Oscillation and has about half the magnitude shown here (although it should be noted that HiGEM is somewhat different in terms of model details, including resolution, compared to the KCM).

3 Methods

The model experiments are listed in Table 1. The control simulation (Experiment CTRL) uses the KCM's standard configuration without any form of correction. Experiment C-FFC is the same as Experiment CTRL except that a flow field correction is applied to the horizontal momentum equations to adjust the path of the North Atlantic Current. Experiment C-FS0 is the same as Experiment C-FFC, including the flow field correction, except that an additional correction is made to the surface freshwater flux seen by the ocean model to bring the model SSS close to climatology. Likewise, Experiment C-FST is the same as Experiment C-FFC except that both the surface freshwater flux and the surface heat flux seen by the ocean model are corrected to bring both the model SSS and SST close to climatology. It should be noted that the method of deriving the corrections (where applied) is the same for the different experiments, but the correction fields themselves are derived separately for each experiment. Hence, the correction to the freshwater flux in C-FST is different from that in C-FS0 and also the flow field corrections in each of Experiments C-FFC, C-FS0 and C-FST are different from each other, as explained below. Additionally, we also make use of Experiment C-0ST in which only the surface fluxes have been corrected (as in traditional flux correction) and no correction is made to the flow field.

3.1 The flow field correction

To correct the spurious path of the NAC and to re-establish a northwest corner in the KCM, we apply a correction to the horizontal momentum equations, leaving the model temperature and salinity equations unchanged, and only altering the model currents by a changed baroclinic pressure gradient. The method is an adaption of the "corrected-prognostic" method introduced by Eden et al. (2004) and is derived from the semi-prognostic method of Sheng et al. (2001) and Greatbatch et al. (2004). In a first step, we alter the horizontal pressure gradient in the model momentum balance by replacing the instantaneous density variable in the model hydrostatic equation by a linear combination of model density, ρ_m, and an input density, ρ_i:

$$\frac{\partial p}{\partial z} = -g\,[\alpha\rho_m + (1-\alpha)\rho_i] \tag{1}$$

which can also be written as

$$\frac{\partial p}{\partial z} = -g\,[\rho_m + (1-\alpha)(\rho_i - \rho_m)] \tag{2}$$

Here, p is pressure and z is the vertical coordinate measured positive upwards. This is a flow-interactive correction, as for each time step, the new density seen in the hydrostatic equation depends on the difference $(\rho_i - \rho_m)$ between model density and input density. It should be noted that the model density itself is calculated from model potential temperature, T, and salinity, S, at the current time step, using the equation of state carried by the model, as in the uncorrected model.

For the input density ρ_i, it is important to use model-compatible temperature and salinity data in order to avoid generating an unrealistic and noisy Joint Effect of Baroclinicity And Relief (JEBAR) term (see, for example, Mellor et al. 1982) due to mismatches between the input hydrographic data and the model topography. To do this, we use the robust

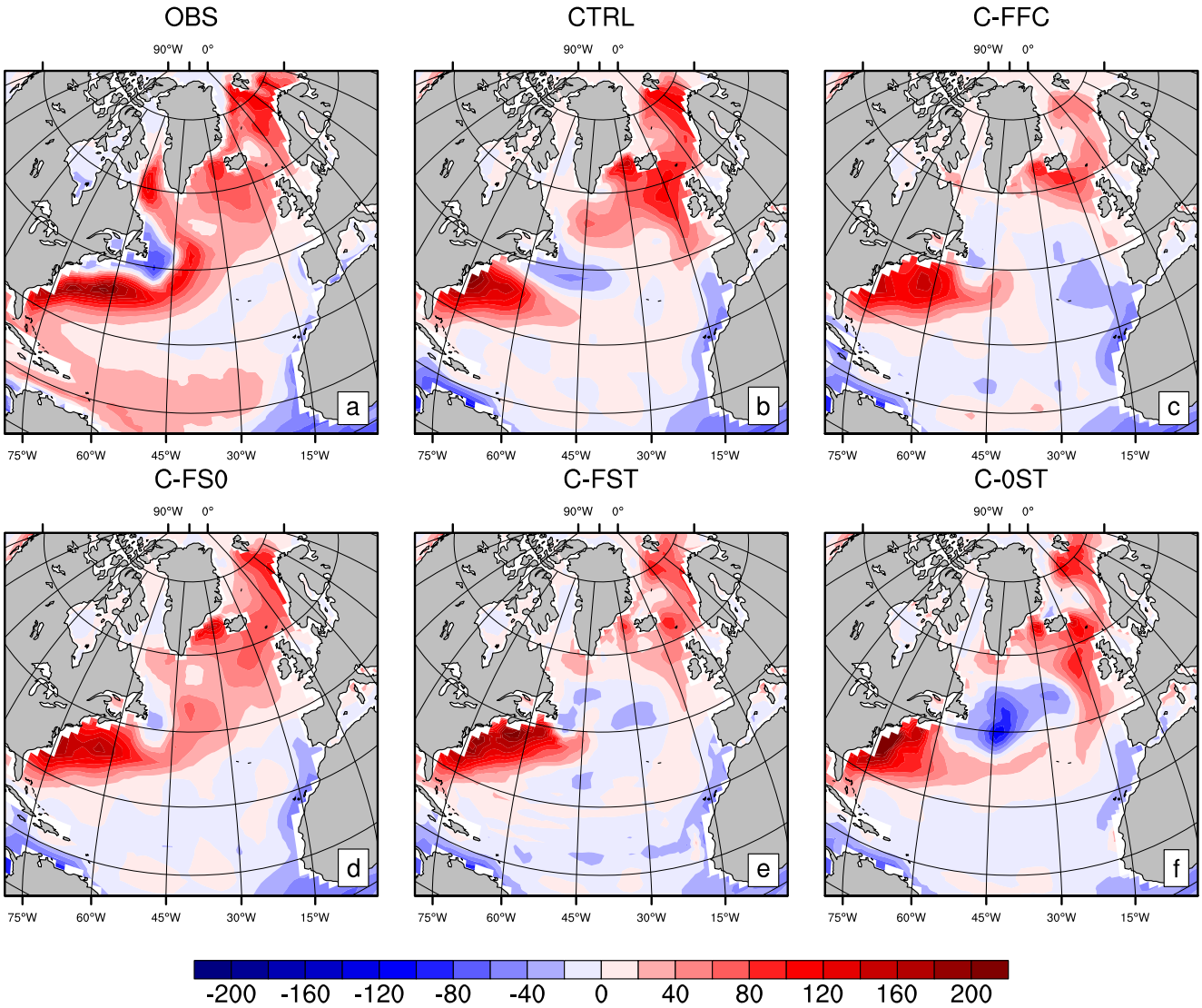

Fig. 4 Mean heat flux (W/m^2) from the ocean to the atmosphere **a** as observed (NCEP, 1948–2012), **b** as in CTRL, **c** C-FFC, **d** C-FS0, **e** C-FST and **f** C-0ST. For the heat flux-corrected experiments, the plotted heat flux includes the correction

diagnostic technique (three-dimensional restoring) that is discussed by Sarmiento and Bryan (1982) as applied to the uncorrected KCM. In the upper 1033 m of the ocean model, Newtonian damping terms of the form:

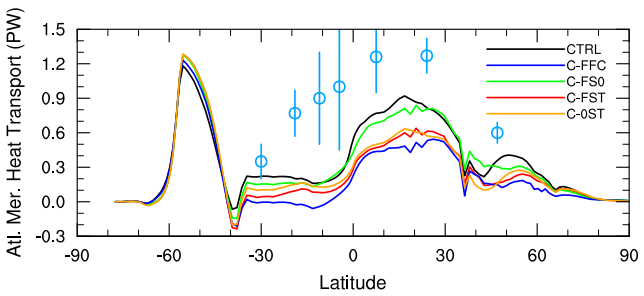

Fig. 5 Atlantic northward heat transport for the control run (*black*) and the corrected runs. *Blue dots* and *error bars* are observed estimates from Ganachaud and Wunsch (2003)

$$\frac{\partial T}{\partial t} = \ldots - \gamma_{3D}(T - T_c) \tag{3}$$

and

$$\frac{\partial S}{\partial t} = \ldots - \gamma_{3D}(S - S_c) \tag{4}$$

are added globally in order to draw the model T and S fields close to the observed climatology, represented by the T_c and S_c fields while still retaining some freedom for the T and S fields to adapt to the model bottom topography. Here, we use the Levitus monthly climatology (Levitus et al. 1998) for the observational fields T_c and S_c, interpolated to model

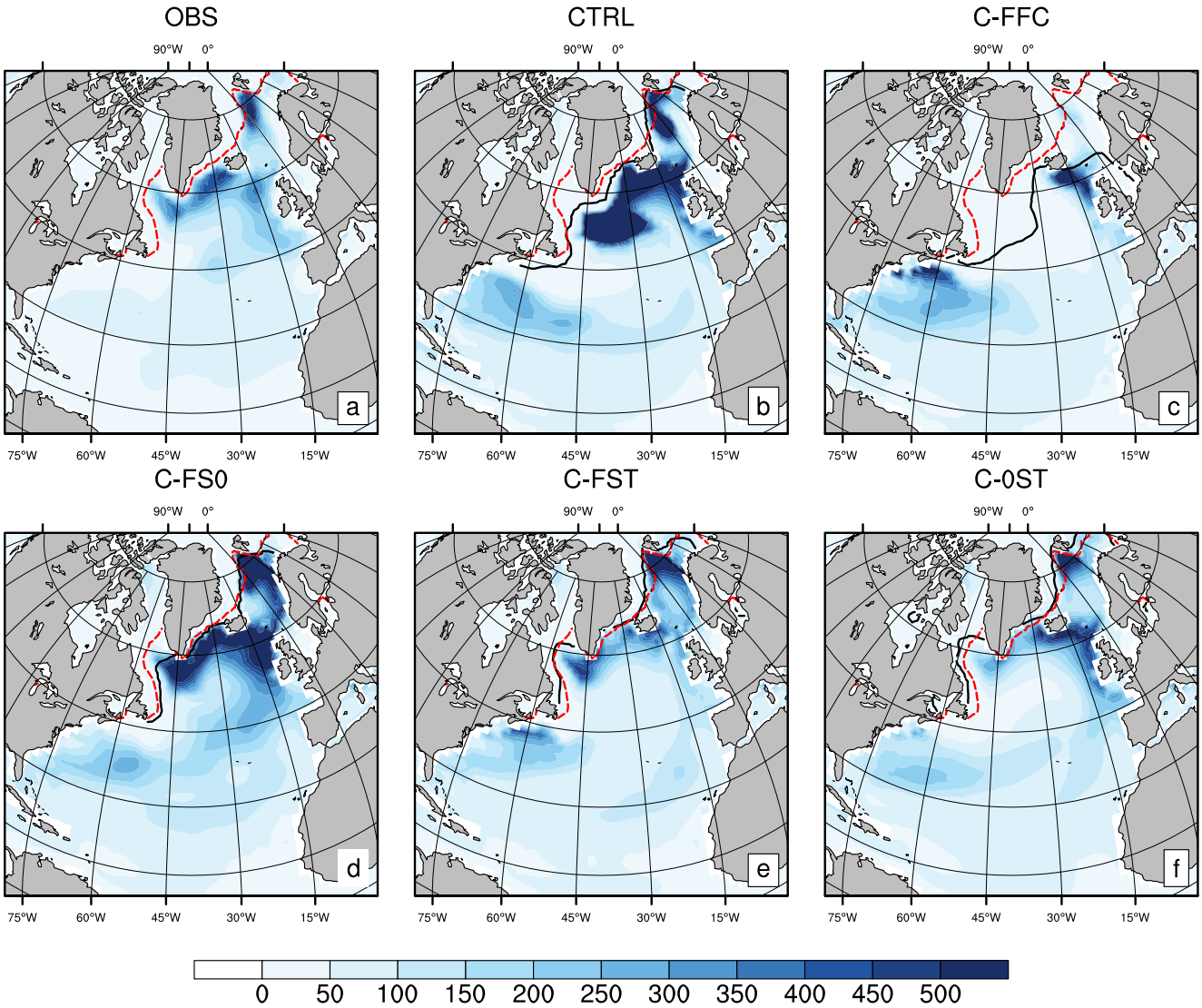

Fig. 6 Winter (January/February/March (JFM)) mean mixed layer depth and March sea ice extent **a** as in the Levitus World Ocean Atlas 1994 (calculation of mixed layer depth described in Monterey and Levitus 1997) and for Experiments **b** CTRL, **c** C-FFC, **d** C-FS0, **e** C-FST and **f** C-0ST. *Colours* show JFM mean mixed layer depth (m), *black contours* denote the March mean of the 15 % sea ice extent, and *red dashed contours* are the March mean 15 % sea ice extent as given by HadISST (1948–2013). In the model, the MLD is defined as the depth at which the potential density referenced to the surface becomes 0.01 kg m^{-3} greater than at the surface

time steps, and the relaxation time scale is 30 days. The robust-diagnostic model version is run for 110 years and output of T and S from the last 50 years is used to calculate a monthly climatology. The input density ρ_i is then computed from this new climatology of T, S using the model equation of state.

3.1.1 Choice of α and localisation

Different choices for the strength of the flow field correction, i.e. the parameter α, can be made. We conducted several experiments with values of 0, 0.3, 0.5 and 0.7 for α. The case $\alpha = 0$, corresponding to a "diagnostic" model, means that the horizontal flow field is determined entirely by the input density except for the vertically averaged barotropic component. In order to maximise the correction, we focus on the diagnostic case and set $\alpha = 0$ in the North Atlantic between 20° and 60°N with a transition zone between 14° and 20°, and 60° and 75°N. Outside of this region, $\alpha = 1$, corresponding to the uncorrected model, and the transition zones are such that α is continuous and varies linearly over the transition zone from 0 to 1. Finally, the flow field correction is applied only from the surface down to a specified cut-off depth. Model runs with different cut-off depths were conducted and the choice of 732 m used here gave the best results.

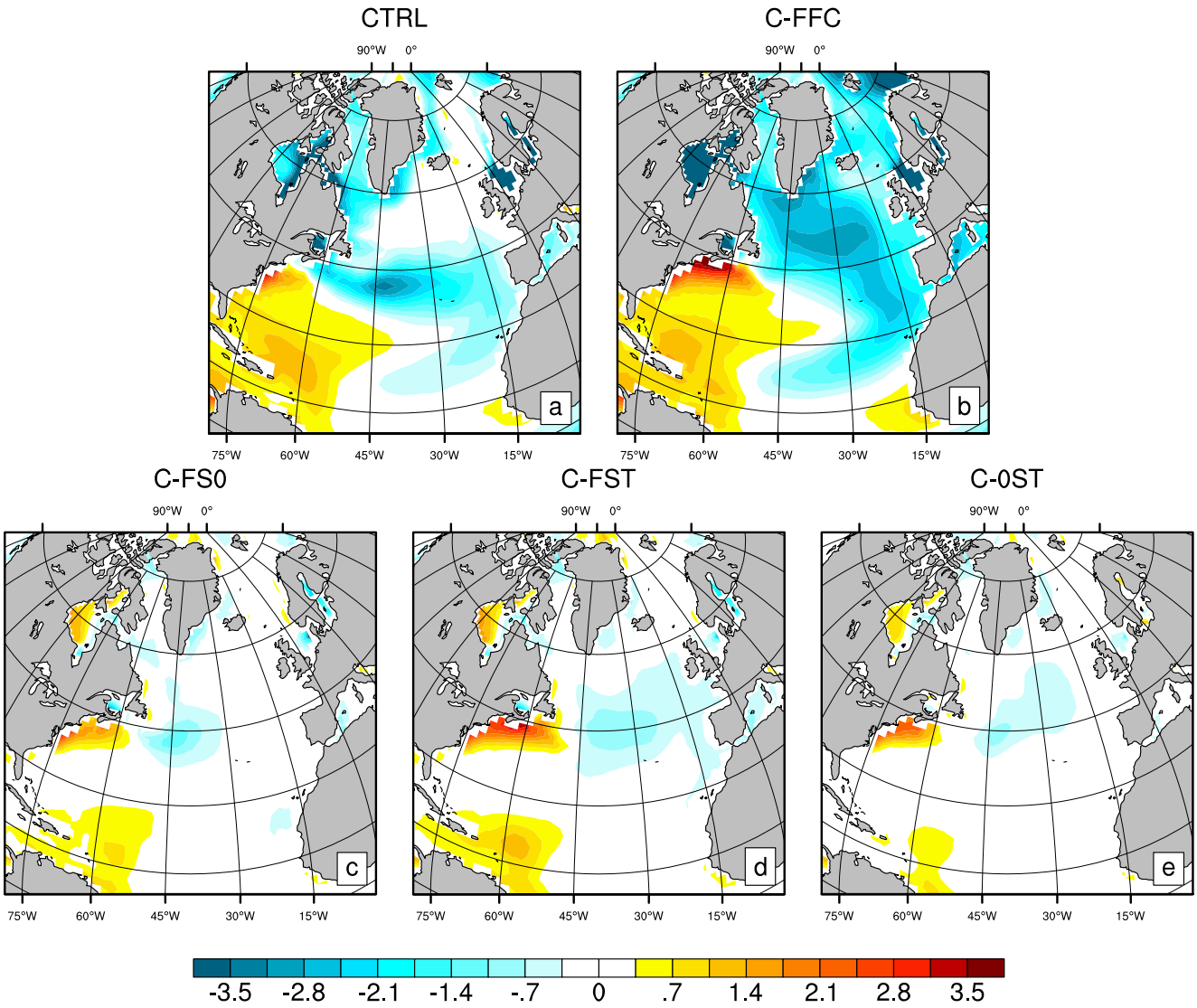

Fig. 7 SSS bias (PSU) of **a** Experiment CTRL, **b** Experiment C-FFC, **c** Experiment C-FS0, **d** Experiment C-FST and **e** Experiment C-0ST, using the WOA (Levitus et al. 1998) as the reference data set

3.1.2 The non-flow interactive correction

Eden et al. (2004) elaborated some disadvantages of the original semi-prognostic method. Among these disadvantages are changed wave dynamics, e.g. reduced Rossby wave speeds and damped eddy activity. These drawbacks can be avoided by making the correction non-flow interactive (as in what Eden et al. (2004) call the "corrected-prognostic method"). In particular, in Eq. 2, the correction appears as the term $(1-\alpha)(\rho_i - \rho_m)$. This term is diagnosed as long-term monthly means from the last 50 years of the previous flow-interactive runs (see Table 1). Re-inserting the diagnosed term in place of the flow-interactive correction term in Eq. 2 then provides a non-flow interactive correction. Throughout the remainder of this paper, "flow field correction" refers to the use of the non-flow interactive correction described here. The correction term can be regarded as a correction for model error and also as a parameterisation of unresolved processes in the momentum balance, one obvious candidate being convergence of the eddy momentum flux.

It is important to note that even though α is set to zero in some regions in the flow-interactive runs (noting that putting $\alpha = 0$ in these runs means that the ocean model is diagnostic), the ocean component of the KCM in the non-flow interactive runs is fully prognostic and is free to evolve everywhere in the model domain. For example, in Experiment C-FFC, the only difference in the model code from Experiment CTRL is the presence of the non-flow interactive correction term.

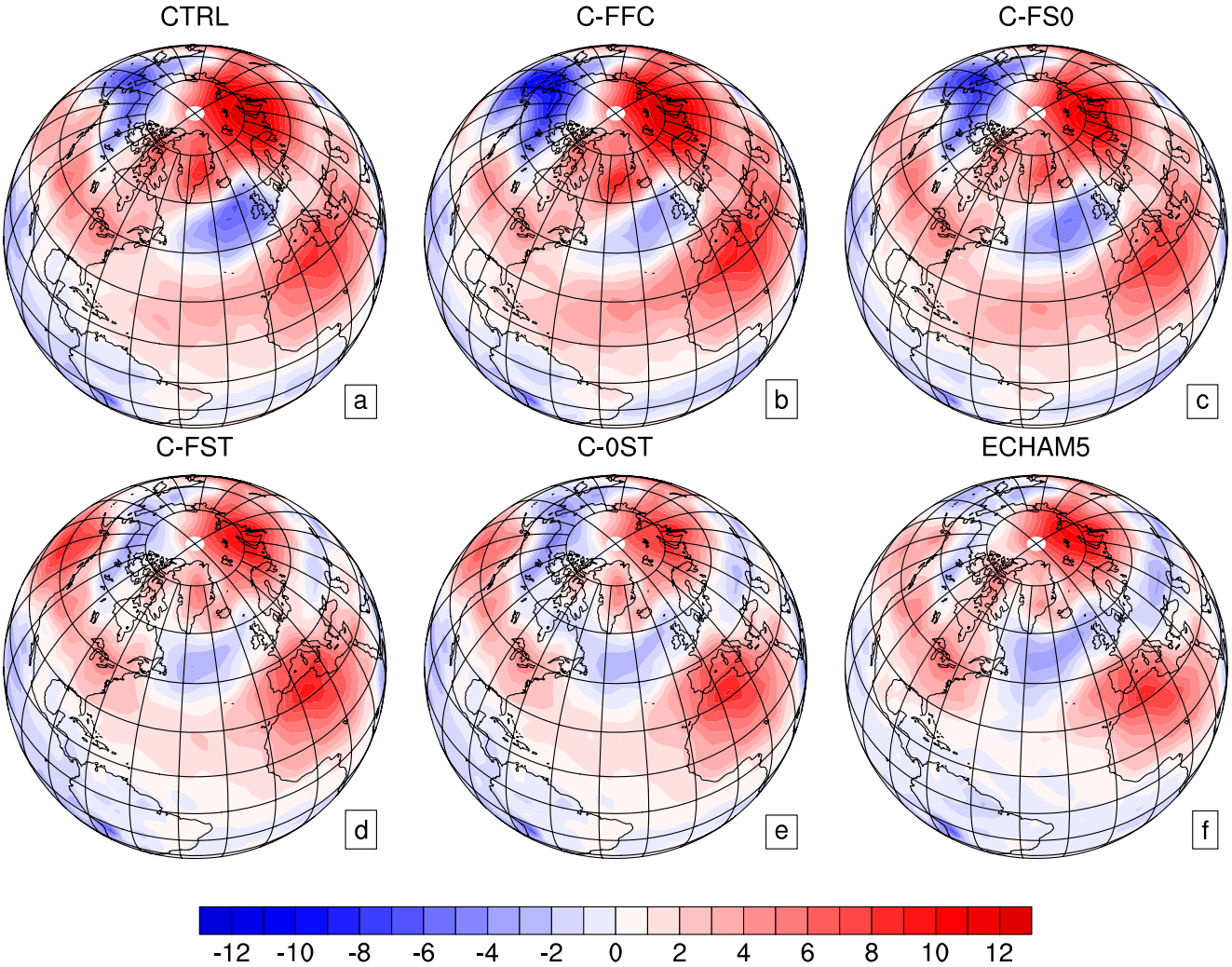

Fig. 8 Sea level pressure bias (hPa) of **a** the control simulation; **b–e** Experiments C-FFC, C-FS0, C-FST and C-0ST and **f** a stand-alone ECHAM5 simulation (see text for details) for the winter (DJF) mean, using ERA-40 reanalysis (1957–2002) as the reference data set

3.2 Surface Correction

To examine the role of inconsistencies in the surface fluxes of freshwater and heat, we set up three more experiments (see Table 1). In Experiment C-FS0, in addition to the use of the flow field correction, the surface freshwater flux is corrected to bring the model SSS close to the SSS in the Levitus monthly mean climatology. In order to do this, a relaxation term $-\gamma(S - S_c)$ is added globally to the salinity equation in the surface level of the model with a relaxation time scale of 30 days.[2] The model is run using this relaxation term concurrently with the flow-interactive flow field correction, the latter being implemented in the same way as in Experiment C-FFC. Both correction terms are then diagnosed simultaneously from this model run as 50-year monthly means. The diagnosed corrections are then used to replace the flow-interactive corrections so that the correction terms in Experiment C-FS0 are non-flow interactive.

In Experiment C-FST, an additional correction to the surface heat flux is made in order to bring the model SST close to the Levitus monthly mean climatology. This means that in addition to the flow-interactive flow field correction and the relaxation term $-\gamma(S - S_c)$ that is added to the salinity equation in the surface level, a relaxation term $-\gamma(T - T_c)$ is also added globally to the equation for the potential temperature in the surface level of the model, again with a relaxation time of 30 days. All three correction terms are then diagnosed simultaneously as monthly means and these three correction terms are then used as non-flow interactive corrections in Experiment C-FST.

We also make use of Experiment C-0ST in which the surface freshwater and heat fluxes are adjusted as in traditional flux correction (e.g. Manabe and Stouffer 1988;

[2]This is for a model with a surface level of depth 5 m.

Sausen et al. 1988). In this case, the model is first run using the relaxation terms $-\gamma(S - S_c)$ and $-\gamma(T - T_c)$ applied globally in the surface level of the model. The relaxation terms are then diagnosed and the diagnosed, non-flow interactive corrections are used in the experiment. It should be noted that no flow field correction is applied in Experiment C-0ST.

Finally, we note that, for the results presented here, the global average of each surface flux correction is removed.

3.3 Experimental strategy

All experiments are initialised with the Levitus potential temperature (T) and salinity (S) monthly climatology (Levitus et al. 1998) in the ocean model on January 1. As noted earlier, the first simulation, the one that uses three-dimensional restoring, was run for 110 years, of which the last 50 years were taken to construct the input density field ρ_i.

The interactive simulations are initialised with the Levitus climatology and corrected using the input density ρ_i as described above. The simulations were run in interactive mode for 249 (C-FS0) and 549 years (C-FFC, C-FST, C-0ST). The simulations are almost equilibrated after this time in the upper ocean. Differences in run times are due to the available computer resources and are not important here. Data from the last 50 years of the interactive simulations are extracted and used to diagnose the corrections for the respective non-interactive simulations, which are initialised with the Levitus climatology. For all non-flow interactive experiments, years 31 to 199 are used for the analysis, while the first 30 years are neglected to avoid the initial adjustment period. See Table 1 for an overview of the different experiments.

4 Results

4.1 Experiment C-FFC: flow field correction alone

Here, we describe the results from Experiment C-FFC in which only a correction to the flow field is applied. It should be remembered when interpreting these results that although α was set to zero for the flow-interactive run used to derive the correction, here the correction is fully non-interactive and the model is free to develop a different flow field from that in the flow-interactive run.

We begin by noting the improvement to the flow field, illustrated by the SSH shown in Fig. 1c. The model now exhibits the typical indentation east of Newfoundland associated with the northwest corner but with the disadvantage that there is an anomalously strong southward extending tongue of relatively low sea level along the east coast of Europe. In the northwest corner itself, the surface cold bias is reduced (see Fig. 2b) and, in fact, a warm bias is now found south of Atlantic Canada associated with the too northward path of the Gulf Stream in the model. However, we can see from Fig. 2b that while the SST bias is reduced in the northwest corner, a surface cold bias remains in the model but is now shifted to the northeast and occupies much of the subpolar North Atlantic and the Nordic Seas. However, in contrast to Experiment CTRL in which the surface cold bias extends down to 1000 m depth, as noted in Section 2, the subpolar cold bias in Experiment C-FFC is shallow. This is illustrated in Fig. 9 which shows the bias in potential temperature at 273 m depth in the model. While a strong cold bias at this depth east of Newfoundland is evident in Experiment CTRL, in Experiment C-FFC, there is instead a weak warm bias in the subpolar North Atlantic (consistent with a weakening of the subpolar gyre circulation compared to CTRL). Comparing with Experiment C-0ST, in which there is no flow field correction but instead the surface fluxes of freshwater and heat are corrected, we see that the flow field correction is necessary to remove the subsurface cold bias; in Experiment C-0ST (see Fig. 9e), the cold bias is still present and large (up to 6 °C) at 273 m depth, despite the fact that the bias in both SST and SSS is greatly reduced (see Figs. 2 and 7).

4.2 Experiments C-FS0 and C-FST: adding surface flux corrections

As can be seen from Fig. 2c, correcting the freshwater flux in addition to the flow field in Experiment C-FS0 leads to a much improved SST field. There is still a cold bias throughout the North Atlantic but this is much less severe than in Experiment CTRL or Experiment C-FFC, although with a magnitude of several degrees Celsius over wide areas. This shows that while correcting the flow field alone, as in Experiment C-FFC, is not sufficient to remove the bias at the surface in the KCM (only to move its location), making an additional correction to the freshwater flux considerably alleviates the bias in SST, despite the fact that in Experiment C-FS0, there is no correction applied to the surface heat flux. In Experiment C-FST, the surface heat flux is corrected as well as the surface freshwater flux and consequently the SST bias is relatively weak in this case. The potential temperature bias at 273 m (see Fig. 9) is, if anything slightly greater than in Experiment C-FS0; otherwise, these two experiments are rather similar.

4.3 The Atlantic Meridional Overturning Circulation (AMOC) and the poleward heat transport

Figure 10 shows the overturning streamfunction in each of the model experiments. The strongest overturning is found

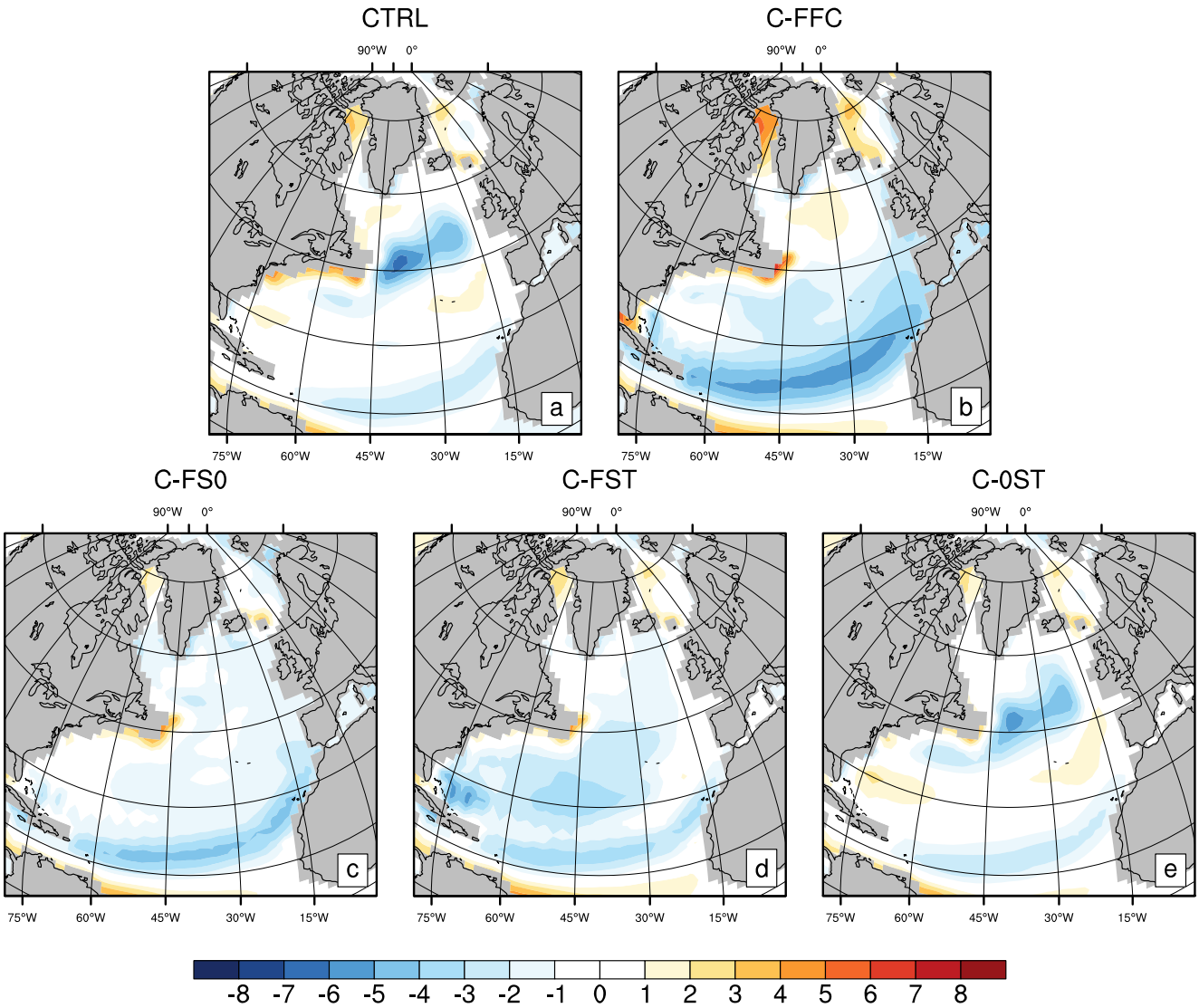

Fig. 9 Potential temperature biases (°C) at 273 m depth of **a** the KCM control experiment (CTRL), **b** Experiment C-FFC, **c** Experiment C-FS0, **d** Experiment C-FST and **e** Experiment C-0ST, using the WOA (Levitus et al. 1998) as the reference data set

in Experiment CTRL, the uncorrected model version, and the weakest in Experiment C-FFC, the case that uses only a flow field correction. As can be seen from Fig. 6, the region where deep convection occurs is much reduced in this experiment compared to Experiment CTRL. Looking at Fig. 11, we see that the surface freshwater flux in Experiment C-FFC is actually quite similar to that in Experiment CTRL in both spatial pattern and magnitude, and that in both experiments there is a bias towards putting too much freshwater into the surface of the subpolar gyre region compared to observations. Since the AMOC is, nevertheless, weak in Experiment C-FFC compared to Experiment CTRL, it seems that in Experiment C-FFC, the circulation is not strong enough to bring sufficient warm and salty water northward to counter the stabilising effect of the surface freshening associated with the freshwater flux over the subpolar gyre region, leading to the weak AMOC in this case.[3] It is notable that the cold bias in this experiment is surface-confined, and coincident with a strong fresh bias in SSS (see Fig. 7). Furthermore, as we noted earlier, the surface cold

[3] Another way of putting this would be to say that the introduction of the flow field correction pushes the model from the model state in CTRL towards a state with a collapsed AMOC, despite the fact that the pattern of the surface freshwater flux is basically the same in both experiments. The reason is probably because of the changed flow path at the surface in C-FFC compared to CTRL that can be seen from Figure 1. In C-FFC, the surface flow path passes under the region of largest freshwater input, as can be seen by comparing Fig. 1 with Fig. 6, whereas in CTRL the flow tends to go around the region of largest freshwater input. This means that the surface flow experiences more freshwater input in C-FFC than in CTRL.

bias is replaced by a warm bias at 273 m depth (see Fig. 9), indicating that the origin of the surface bias is the surface freshwater flux and not the misplaced circulation. In Experiment CTRL, on the other hand, the region of the cold bias is also characterised by a fresh bias in salinity at the surface but in this case, the cold bias is deep (extending down to 1000 m), indicating that the misplaced circulation has an important role to play in its dynamics. It is also notable that in Experiment C-FFC, there is a weakening of the biases in both SST and SSS in the region between the British Isles and Iceland where convection is taking place in Experiment C-FFC (see the deepened mixed layer depth in this region in Fig. 6c). It is only here that the surface freshwater input is being mixed down by the convection and, correspondingly, heat is being mixed up to the surface. Importantly, Experiment C-FS0 shows a robust AMOC and differs from Experiment C-FFC only in the surface freshwater flux.

An interesting feature of Experiments C-FS0 and C-FST is the strengthening of the AMOC north of 40° N compared to Experiment CTRL, suggesting a role for the flow field correction in extending the northward penetration of the AMOC (see Fig. 10f for an example). In general, the overturning cell associated with North Atlantic deep water tends to be shallower and weaker than in Experiment CTRL, the exception being Experiment C-FS0. This is true of both experiments that correct the surface heat flux (C-FST and C-0ST). This weakening of the AMOC is associated with a bias towards too little heat loss over the subpolar North Atlantic in these experiments (Fig. 4) and weakening of the deep convection in the subpolar North Atlantic compared to Experiments CTRL and C-FS0—see Fig. 6 and note the reduced mixed layer depths in Experiments C-FST and C-0ST in the subpolar North Atlantic. It is also notable that in all the experiments that correct the surface fluxes, the deep convection site is shifted, compared to Experiment CTRL, into the Labrador Sea. This is true even in Experiment C-0ST that does not use a flow field correction and also in Experiment C-FS0 that uses a flow field correction but only corrects the freshwater flux. It follows that the lack of deep convection in the Labrador Sea in the KCM is due to the inability of the surface freshwater flux in the KCM to ensure the correct SSS. It is also notable that in those model runs that support deep convection in the Labrador Sea, the representation of sea ice in the Labrador Sea is much improved (Fig. 6). In Experiment CTRL, the Labrador Sea is largely ice covered in winter, whereas in Experiments C-FS0, C-FST and C-0ST, the ice edge is much more realistically located.

Turning to the poleward heat transport (see Fig. 5), we first note that all model cases, including Experiment CTRL, carry a lower ocean heat transport in the Atlantic than what is observed. Between experiments, it is not surprising that the strength of the poleward heat transport goes along with the strength of the AMOC, the strongest being

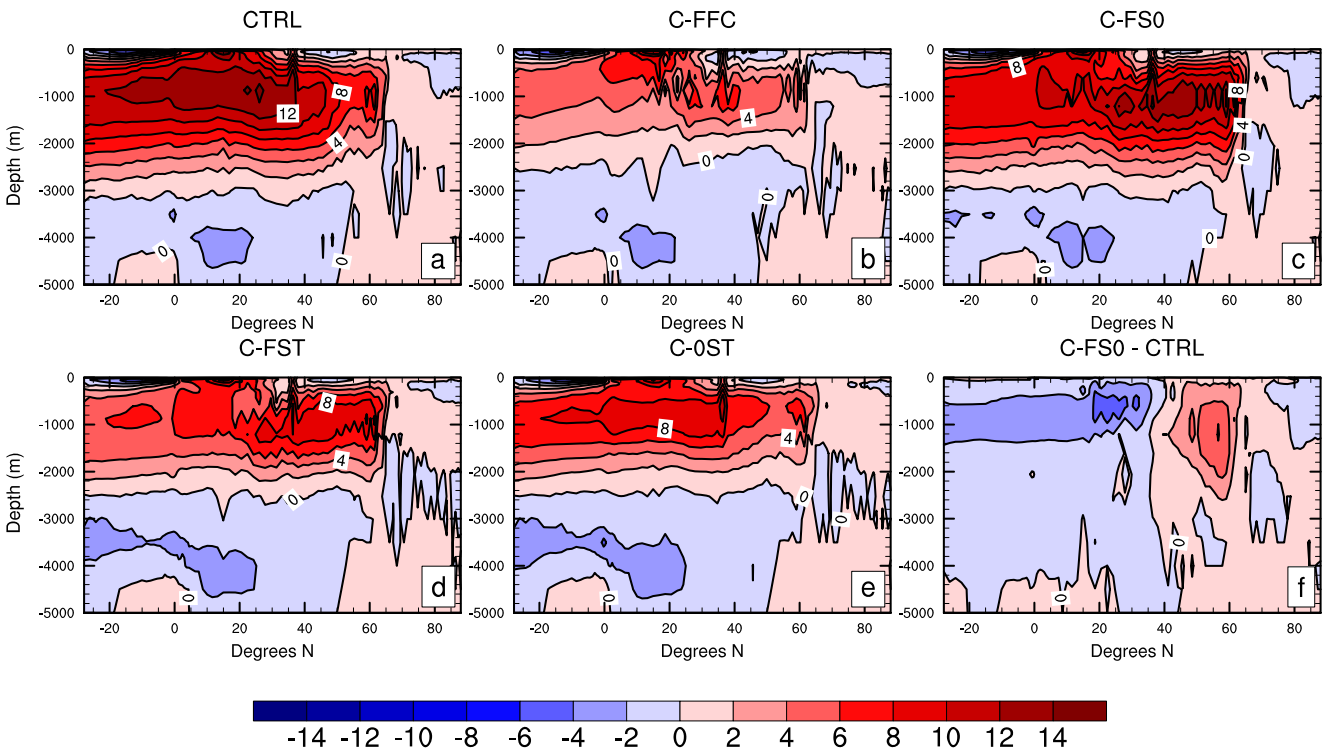

Fig. 10 The time mean Atlantic meridional overturning streamfunction (Sv) from **a** the control run, **b**–**e** Experiments C-FFC, C-FS0, C-FST and C-0ST, respectively. **f** Shows the difference C-FS0 minus CTRL

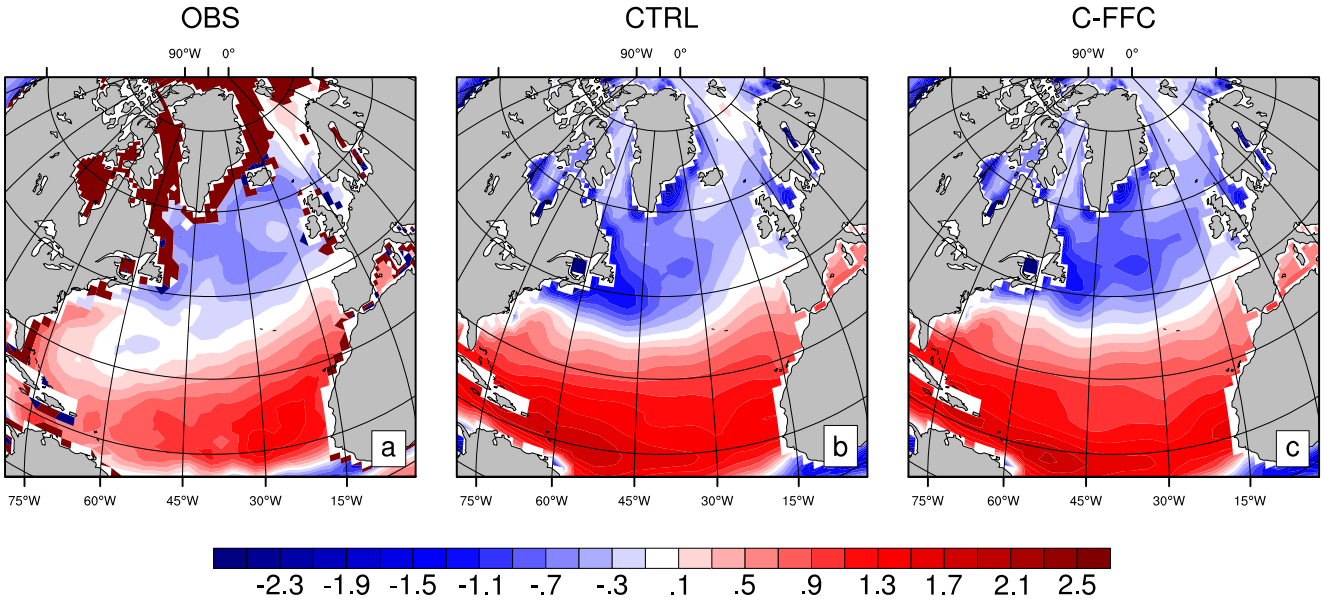

Fig. 11 Surface fresh water flux into the ocean (m/year) **a** as observed (NOC1.1 climatology, NOC, Southampton), **b** in Experiment CTRL and **c** in Experiment C-FFC

in Experiment CTRL and the weakest in Experiment C-FFC. Of the cases that correct the surface fluxes as well as the flow field, the strongest poleward heat transport is found in Experiment C-FS0 that corrects the surface freshwater flux, but not the heat flux, as one would have expected based on the AMOC strength. Another feature of the poleward heat transport is the erroneous bump near 50° N in Experiments CTRL and C-0ST (those cases that do not use the flow field correction) that arises from the strong heat input to the ocean model over the region of the cold bias (see Fig. 4). In the flow field corrected experiments, this bump is much smaller or even eliminated (in C-FS0), as the re-establishment of the northwest corner removes the spurious heat input that is otherwise trying to remove the cold bias.

4.4 The atmospheric circulation

The bias in the atmospheric circulation in the KCM is strongest in the winter season (December/January/February (DJF)) and for that reason, we focus on the winter season in what follows. Figure 8 shows the winter mean sea level pressure (SLP) biases in the model experiments, using the ERA-40 reanalysis for the period 1957 to 2002 as the reference data set. It is clear from Fig. 8 that the bias in all experiments is hemispheric in extent (it is not confined solely to the North Atlantic). Also, a similar bias (not shown) is found at 500 hPa. As noted in Section 2, in Experiment CTRL (the uncorrected KCM), the SLP bias can be as much as 10 hPa in the North Atlantic sector and strongly projects onto the East Atlantic pattern (Barnston and Livezey 1987). In Experiments C-FST and C-0ST, which correct both the surface heat and freshwater fluxes, the bias is still present although reduced to about half the magnitude east of the British Isles. In these experiments, the bias is very similar that in a stand-alone ECHAM5 run of the same resolution as in Experiment CTRL and using climatological SST and sea ice at the lower boundary (see Fig. 8f), showing that the origin of the bias shown here is in the atmospheric model. A disappointing feature is that, of the corrected models, the bias is reduced the least in Experiment C-FS0, the case that corrects both the flow field and the surface freshwater water flux, and which gives the best performance in the ocean model. The reason for this is unclear but perhaps is related to the general surface cooling in this case that can be seen in Fig. 2c (this cooling is actually hemispherical in extent—not shown). It should be noted that the bias in SLP is not changed in Experiments CTRL, C-FS0 and C-FST when 1000 years of model output are used.

5 Summary and discussion

We have described the use of empirical correction techniques designed to alleviate the North Atlantic cold bias that is a ubiquitous feature of coupled atmosphere/ocean/sea ice climate and forecast models (Wang et al. 2014). The cold bias is typically associated with a too zonal path of the North Atlantic Current from Newfoundland towards Europe. The new feature here is the use of a flow field correction to adjust the path of the North Atlantic Current in order to recover the northwest corner (Lazier 1994). Applied to the Kiel Climate Model (KCM), we found that the flow field correction almost completely eliminates the subsurface cold bias (in

the uncorrected KCM, the cold bias extends down to a depth of 1000 m) leaving a shallow cold bias at the surface that is displaced northeastward from the location of the cold bias in the uncorrected model. This cold bias is, in turn, largely removed by correcting the surface freshwater flux seen by the ocean model without any need to additionally correct the surface heat flux. Interestingly, we also found that in an experiment that corrects only the surface freshwater and heat fluxes, but does not include a flow field correction, the bias remains in the subsurface with almost the same magnitude as in the uncorrected model. This shows that the flow field correction is essential for removing the bias. We conclude that in the KCM, the surface cold bias has two main origins. One is the misplacement of the North Atlantic Current in the model and the other is the inability of the surface freshwater flux to bring the model surface salinity close to the observed surface salinity.

An important aspect of the flow field correction is that it is non-flow interactive. This means that, in a linear sense, there is no corruption of the dynamics within the ocean model through application of the correction. Furthermore, because it is applied only to the model momentum equation, there are no sources and sinks of heat and salt introduced by the method. Another important feature of the method is a preliminary adjustment that is made to the input data (in this case, the Levitus climatology) in order to ensure that the input data are compatible with the model geometry (in particular, the bottom topography), avoiding issues with the JEBAR term (see, for example, Mellor et al. 1982).

We also noted that in the KCM, the atmospheric bias over the North Atlantic strongly projects onto the East Atlantic pattern with a low surface pressure bias over and to the west of the British Isles, rather than the NAO, as reported by Keeley et al. (2012) in the case of the HiGEM model. In those experiments that include a correction to the surface heat flux, the bias was generally reduced east of the British Isles (but not significantly changed at other locations). However, Experiment C-FS0, that corrects the flow field and the surface freshwater flux only, exhibits a bias very similar to that in the uncorrected KCM. We do not know why the atmospheric bias shows no reduction in this case but suggest that it could be related to the general cooling of the northern hemisphere (not shown) in this experiment.

A particularly unfortunate consequence of the cold bias is the reversed direction of the surface heat flux in a region of the North Atlantic thought to be important for influencing European climate (e.g. Rodwell and Folland 2002); instead of the atmosphere taking up heat from the ocean, the atmosphere is losing heat to the ocean in an effort to counter the bias. It is, therefore, perhaps not surprising that experience at the UK Met Office strongly suggests that improved seasonal forecasts over the North Atlantic are possible in a model with a reduced North Atlantic cold bias (Scaife et al. 2014, Scaife, personal communication). However, the cold bias has proved hard to eliminate in coupled models; even some very high-resolution coupled models still exhibit a bias as strong as in a lower resolution version of the same model (see Figure 2 in Delworth et al. 2012). We feel, therefore, that the empirical techniques discussed here offer a pragmatic means of reducing the bias and improving the utility of coupled models, for example, for seasonal and decadal forecasting. Nevertheless, because the corrections are tuned for a present day climate, it is not clear that they should be used for long-term climate change projections or for palaeoclimate modelling in which the model climate state can differ radically from that of today.

Finally, in a future study, we shall compare the variability in the different model versions in detail with a focus on the interdecadal time scales for which the change in the mean background state between the different model versions is expected to have an impact.

Acknowledgments AD is grateful for support through the Helmholtz Graduate School HOSST. Support from the GEOMAR Helmholtz Centre for Ocean Research Kiel, the BMBF MiKlip project ATMOS and the EU NACLIM project is also acknowledged. The authors are also grateful to two anonymous reviewers for their helpful comments on the manuscript.

References

Ba J, Keenlyside NS, Park W, Latif M, Hawkins E, Ding H (2013) A mechanism for Atlantic multidecadal variability, in the Kiel Climate Model. Clim Dyn 41(7-8):2133–2144. doi:10.1007/s00382-012-1633-4

Barnston AG, Livezey RE (1987) Classification, seasonality and persistence of low-frequency atmospheric circulation patterns. Mon Wea Rev 115(6):1083–1126. doi:10.1175/1520-0493(1987)115¡1083:CSAPOL¿2.0.CO;2

Behrens E (2013) The oceanic response to Greenland melting: the effect of increasing model resolution.Universittsbibliothek Kiel, Kiel. http://macau.uni-kiel.de/receive/dissertation_diss_00013684

Born A, Mignot J (2012) Dynamics of decadal variability in the Atlantic subpolar gyre: a stochastically forced oscillator. Clim Dyn 391(2):461–474. doi:10.1007/s00382-011-1180-4

Brayshaw DJ, Hoskins B, Blackburn M (2011) The basic ingredients of the North Atlantic storm track. Part II: Sea surface temperatures. J Atmos Sci 68(8):1784–1805. doi:10.1175/2011JAS3674.1

Bryan FO, Hecht MW, Smith RD (2007) Resolution convergence and sensitivity studies with North Atlantic circulation models. Part I: The western boundary current system, vol 16, pp 141–159. doi:10.1016/j.ocemod.2006.08.005

Delworth T, Manabe S, Stouffer RJ (1993) Interdecadal variations of the thermohaline circulation in a coupled ocean-atmosphere model. J Clim 6(11):1993–2011. doi:10.1175/1520-0442(1993)006¡1993:IVOTTC¿2.0.CO;2

Delworth TL, Rosati A, Anderson W, Adcroft AJ, Balaji V, Benson R, Dixon K, Griffies SM, Lee HC, Pacanowski RC, Vecchi GA, Wittenberg AT, Zeng F, Zhang R (2012) Simulated climate and climate change in the GFDL CM2.5 high- resolution coupled climate model. J Clim 25(8):2755–2781. doi:10.1175/JCLI-D-11-00316.1

Eden C, Greatbatch RJ, Boning CW (2004) Adiabatically correcting an eddy-permitting model using large-scale hydrographic data: application to the Gulf Stream and the North Atlantic Current. J Phys Oceanogr 34(4):701–719. doi:10.1175/1520-0485(2004)034¡0701:ACAEMU¿2.0.CO;2

Flato G, Marotzke J, Abiodun B, Braconnot P, Chou S, Collins W, Cox P, Driouech F, Emori S, Eyring V, Forest C, Gleckler P, Guilyardi E, Jakob C, Kattsov V, Reason C, Rummukainen M (2014) Evaluation of climate models. In: Climate change 2013—the physical science basis. Contribution of Working Group I to the Fifth Assessment Report of the Intergovernmental Panel on Climate Change, Cambridge University Press, pp 741–866. doi:10.1017/CBO9781107415324.020

Folland CK, Scaife AA, Lindesay J, Stephenson DB (2012) How potentially predictable is northern European winter climate a season ahead?, vol 32, pp 801–818. doi:10.1002/joc.2314

Ganachaud A, Wunsch C (2003) Large-scale ocean heat and freshwater transports during the World Ocean Circulation Experiment. J Clim 16(4):696–705. doi:10.1175/1520-0442(2003)016¡0696:LSOHAF¿2.0.CO;2

Gerdes R, Köberle C (1995) On the influence of DSOW in a numerical model of the North Atlantic general circulation. J Phys Oceanogr 25(11):2624–2642. doi:10.1175/1520-0485(1995)025¡2624:OTIODI¿2.0.CO;2

Greatbatch RJ (2000) The North Atlantic Oscillation. Stoch Env Res Risk A 14(4-5):213–242. doi:10.1007/s004770000047

Greatbatch RJ, Fanning AF, Goulding AD, Levitus S (1991) A diagnosis of interpentadal circulation changes in the North Atlantic. J Geophys Res 96(C12):22,009–22,023. doi:10.1029/91JC02423

Greatbatch RJ, Sheng J, Eden C, Tang L, Zhai X, Zhao J (2004) The semi-prognostic method, vol 24, pp 2149–2165. doi:10.1016/j.csr.2004.07.009

Greatbatch RJ, Zhai X, Claus M, Czeschel L, Rath W (2010) Transport driven by eddy momentum fluxes in the Gulf Stream extension region. Geophys Res Lett 24(L24):401. doi:10.1029/2010GL045473

Griffies SM, Winton M, Anderson WG, Benson R, Delworth TL, Dufour CO, Dunne JP, Goddard P, Morrison AK, Rosati A, Wittenberg AT, Yin J, Zhang R (2014) Impacts on ocean heat from transient mesoscale eddies in a hierarchy of climate models. J Clim 28(3):952–977. doi:10.1175/JCLI-D-14-00353.1

Hecht MW, Smith RD (2008) Toward a physical understanding of the North Atlantic: a review of model studies, in an eddying regime. In: Hecht MW, Hasumi H (eds) Ocean modeling in an eddying regime, American Geophysical Union, pp213–239

Hoskins BJ, Valdes PJ (1990) On the Existence of storm-tracks. J Atmos Sci 47(15):1854–1864. doi:10.1175/1520-0469(1990)047¡1854:OTEOST¿2.0.CO;2

Hurrell JW, Kushnir Y, Ottersen G, Visbeck M (2003) An overview of the North Atlantic Oscillation. In: Hurrell JW, Kushnir Y, Ottersen G, Visbeck M (eds) The North Atlantic Oscillation: climatic significance and environmental impact, American Geophysical Union, pp 1–35

Keeley SPE, Sutton RT, Shaffrey LC (2012) The impact of North Atlantic sea surface temperature errors on the simulation of North Atlantic European region climate. QJR Meteorol Soc 138(668):1774–1783. doi:10.1002/qj.1912

Lazier JRN (1994) Observations in the northwest corner of the North Atlantic Current. J Phys Oceanogr 24(7):1449–1463. doi:10.1175/1520-0485(1994)024¡1449:OITNCO¿2.0.CO;2

Levitus S, Boyer T, Conkright M, O'Brien T, Antonov J, Stephens C, Stathoplos L, Johnson D, Gelfeld R (1998) NOAA Atlas NESDIS 18, World Ocean Database. VOLUME 1: INTRODUCTION. U.S. Gov. Printing Office Washington D.C

Madec G (2008) NEMO ocean engine Note du Pole de modélisation. Institut Pierre-Simon Laplace (IPSL), France

Manabe S, Stouffer RJ (1988) Two stable equilibria of a coupled ocean-atmosphere model. J Clim 1(9):841–866. doi:10.1175/1520-0442(1988)001¡0841:TSEOAC¿2.0.CO;2

Mellor GL, Mechoso CR, Keto E (1982) A diagnostic calculation of the general circulation of the Atlantic Ocean, vol 29, pp 1171–1192. doi:10.1016/0198-0149(82)90088-7

Mertens C, Rhein M, Walter M, Böning CW, Behrens E, Kieke D, Steinfeldt R, Stöber U (2014) Circulation and transports in the Newfoundland Basin, western subpolar North Atlantic. J Geophys Res Oceans 119(11):7772–7793. doi:10.1002/2014JC010019

Monterey G, Levitus S (1997) NOAA Atlas NESDIS 14: Seasonal variability of mixed layer depth for the world ocean. U.S.Gov. Printing Office, Washington, D.C.

Park W, Keenlyside N, Latif M, Ströh A, Redler R, Roeckner E, Madec G (2009) Tropical pacific climate and its response to global warming in the Kiel Climate Model. J Clim 22(1):71–92. doi:10.1175/2008JCLI2261.1

Ratcliffe RaS, Murray R (1970) New lag associations between North Atlantic sea temperature and European pressure applied to long-range weather forecasting. QJR Meteorol Soc 96(408):226–246. doi:10.1002/qj.49709640806

Rodwell MJ, Folland CK (2002) Atlantic air–sea interaction and seasonal predictability. QJR Meteorol Soc 128(583):1413–1443. doi:10.1002/qj.200212858302

Rodwell MJ, Rowell DP, Folland CK (1999) Oceanic forcing of the wintertime North Atlantic Oscillation and European climate, vol 398, pp 320–323. doi:10.1038/18648

Roeckner E, Baeuml G, Bonaventura L, Brokopf R, Esch M, Giorgetta M, Hagemann S, Kirchner I, Kornblueh L, Manzini E, Rhodin A, Schlese U, Schulzweida U, Tompkins A (2003) The atmospheric general circulation model ECHAM5—part 1 MPI-Report 349, Max Planck Institute for Meteorology, Hamburg, Gemany

Sarmiento JL, Bryan K (1982) An ocean transport model for the North Atlantic. J Geophys Res 87(C1):394–408. doi:10.1029/JC087iC01p00394

Sausen R, Barthel K, Hasselmann K (1988) Coupled ocean-atmosphere models with flux correction. Clim Dyn 2(3):145–163. doi:10.1007/BF01053472

Scaife AA, Copsey D, Gordon C, Harris C, Hinton T, Keeley S, O'Neill A, Roberts M, Williams K (2011) Improved Atlantic winter blocking in a climate model. Geophys Res Lett 38(23):L23,703. doi:10.1029/2011GL049573

Scaife AA, Arribas A, Blockley E, Brookshaw A, Clark RT, Dunstone N, Eade R, Fereday D, Folland CK, Gordon M, Hermanson L, Knight JR, Lea DJ, MacLachlan C, Maidens A, Martin M, Peterson AK, Smith D, Vellinga M, Wallace E, Waters J, Williams A (2014) Skillful long-range prediction of European and North American winters. Geophys Res Lett 41(7):2014GL059,637. doi:10.1002/2014GL059637

Schott FA, Fischer J, Dengler M, Zantopp R (2006) Variability of the deep western boundary current east of the Grand Banks. Geophys Res Lett 33(21):L21S07. doi:10.1029/2006GL026563

Sheng J, Greatbatch RJ, Wright DG (2001) Improving the utility of ocean circulation models through adjustment of the momentum balance. J Geophys Res 106(C8):16,711–16,728. doi:10.1029/2000JC000680

Valcke S (2006) OASIS3 User Guide. PRISM technical report. Tech. Rep. TR/CMGC/06/73 CERFACS Toulouse, France

Valcke S (2013) The OASIS3 coupler: a European climate modelling community software. Geosci Model Dev 6(2):373–388. doi:10.5194/gmd-6-373-2013

Wang C, Zhang L, Lee SK, Wu L, Mechoso CR (2014) A global perspective on CMIP5 climate model biases. Nat Clim Chang 4(3):201–205. doi:10.1038/nclimate2118

Weese SR, Bryan FO (2006) Climate impacts of systematic errors in the simulation of the path of the North Atlantic Current. Geophys Res Lett 19(L19):708. doi:10.1029/2006GL027669